







Identification of a novel fatty acid binding protein-5-CB2 receptor-dependent mechanism regulating anxiety behaviors in the prefrontal cortex

Taygun C. Uzuneser ¹, Hanna J. Szkudlarek ¹, Matthew J. Jones¹, Mina G. Nashed ¹, Timothy Clement^{2,3}, Hehe Wang ^{2,3}, Iwao Ojima ^{2,3}, Walter J. Rushlow^{1,4}, Steven R. Laviolette ^{1,4,*}

¹Department of Anatomy and Cell Biology, Schulich School of Medicine and Dentistry, 1151 Richmond Street, Medical Sciences Building, University of Western Ontario, London, ON N6A 3K7, Canada,

²Institute of Chemical Biology and Drug Discoveries, 100 Nicolls Road, Stony Brook University, Stony Brook, NY 11794-3400, United States,

³Department of Chemistry, 100 Nicolls Road, Stony Brook University, Stony Brook, NY 11794-3400, United States,

⁴Department of Psychiatry, Schulich School of Medicine and Dentistry, 1151 Richmond Street, Mental Health Care Building, University of Western Ontario, London, ON N6A 3K7, Canada

*Corresponding author: Department of Anatomy and Cell Biology, University of Western Ontario, 468 Medical Science Building, London, ON N6A 3K7, Canada. Email: steven.laviolette@schulich.uwo.ca

The endocannabinoid (eCB) system represents a promising neurobiological target for novel anxiolytic pharmacotherapies. Previous clinical and preclinical evidence has revealed that genetic and/or pharmacological manipulations altering eCB signaling modulate fear and anxiety behaviors. Water-insoluble eCB lipid anandamide requires chaperone proteins for its intracellular transport to degradation, a process that requires fatty acid-binding proteins (FABPs). Here, we investigated the effects of a novel FABP-5 inhibitor, SBFI-103, on fear and anxiety-related behaviors using rats. Acute intra-prelimbic cortex administration of SBFI-103 induced a dose-dependent anxiolytic response and reduced contextual fear expression. Surprisingly, both effects were reversed when a cannabinoid-2 receptor (CB2R) antagonist, AM630, was co-infused with SBFI-103. Co-infusion of the cannabinoid-1 receptor antagonist Rimobant with SBFI-103 reversed the contextual fear response yet showed no reversal effect on anxiety. Furthermore, *in vivo* neuronal recordings revealed that intra-prelimbic region SBFI-103 infusion altered the activity of putative pyramidal neurons in the basolateral amygdala and ventral hippocampus, as well as oscillatory patterns within these regions in a CB2R-dependent fashion. Our findings identify a promising role for FABP5 inhibition as a potential target for anxiolytic pharmacotherapy. Furthermore, we identify a novel, CB2R-dependent FABP-5 signaling pathway in the PFC capable of strongly modulating anxiety-related behaviors and anxiety-related neuronal transmission patterns.

Key words: endocannabinoids; fatty acid binding protein-5; *in vivo* electrophysiology; pharmacotherapy; prelimbic cortex.

Introduction

Endogenous cannabinoid (eCB) signaling has been linked to modulating fear, anxiety, and stress responses, and its dysfunction is implicated in the pathophysiology of psychiatric disorders including schizophrenia, substance abuse, depression, and anxiety disorders (Gunduz-Cinar, MacPherson, et al. 2013a; Garani et al. 2021; Laviolette 2021; Zhang et al. 2021). Anandamide (AEA) and 2-arachidonoyl glycerol (2-AG) are eCB ligands that are synthesized on demand following neuronal activation, are released into the synaptic cleft by diffusion, and activate numerous targets including cannabinoid CB1 receptor (CB1R), CB2 receptor (CB2R), peroxisome proliferator-activated receptor gamma (PPAR γ), and G-protein coupled receptor 55 (GPR55) (Marsicano et al. 2003; Alger and Kim 2011; Fowler 2013). Thereafter, AEA and 2-AG are cleared from the synaptic cleft by cellular uptake and metabolized by fatty acid amide hydroxylase (FAAH) and monoacylglycerol lipase (MAGL), respectively (Blankman and Cravatt 2013). Importantly, pharmacological agents

and genetic manipulations that increase eCB signaling have been shown to reduce anxiety, facilitate fear extinction, and dampen amygdala activation *in vivo* (Chhatwal et al. 2005; Hill et al. 2013; Gunduz-Cinar, MacPherson, et al. 2013a). Pharmacological inhibition of FAAH or AEA uptake has been shown to produce anxiolytic-like effects and facilitate fear extinction in rats (Kathuria et al. 2003; Chhatwal et al. 2005; Zaitone et al. 2012; Lisboa et al. 2015). Furthermore, a key polymorphism in the FAAH gene, which destabilizes the FAAH protein, has been associated with reduced trait anxiety and elevated cortex-amygdala connectivity (Hariri et al. 2009; Gunduz-Cinar, Hill, et al. 2013b; Dincheva et al. 2015).

Water-insoluble eCB lipids require chaperone proteins for their intracellular transport. Research has identified 3 main isoforms of fatty acid binding proteins (FABP) that are expressed in the adult brain; FABP-3, FABP-5, and FABP-7 (Owada et al. 1996; Smathers and Petersen 2011). Kaczocha et al. (2009) identified FABPs as intracellular

transporters for AEA, with FABP-5 and FABP-7 having higher affinities to bind AEA than FABP-3. While the adult brain abundantly expresses FABP-5, FABP-7 expression is down-regulated postnatally (Owada et al. 1996), implicating FABP-5 as the primary transporter of AEA. Intracellularly, FABP-5 binds to AEA and transports it to FAAH, which is localized in the endoplasmic reticulum, for its breakdown (Cravatt et al. 2001; Kaczocha et al. 2009). Thus, similar to the inactivation of FAAH or AEA uptake, inactivation of FABPs results in elevated AEA-mediated neurotransmission without impacting 2-AG levels (Kaczocha et al. 2014; Yu et al. 2014; Yan et al. 2018). Importantly, inhibition of FABP-5 and FABP-7 by systemic SBFI-26 administration results in reduced ethanol consumption (Figueiredo et al. 2017) as well as anti-inflammatory and analgesic effects (Yan et al. 2018) without causing motor or cognitive impairments in mice (Thanos et al. 2016). Furthermore, FABP-5/7 knockout mice demonstrate an antidepressive phenotype (Hamilton et al. 2018) while elevated FABP-5 mRNA levels have been detected in the PFC of postmortem brains of schizophrenia patients (Shimamoto et al. 2014). These findings strongly associate FABP signaling abnormalities with various psychiatric conditions.

Despite the involvement of eCB signaling in many psychiatric conditions, including anxiety disorders, the effects of FABPs on the modulation of fear and anxiety have not been thoroughly investigated. To address this issue, we investigated the behavioral effects of a novel compound, SBFI-103, which is a potent FABP-5 inhibitor with negligible affinities for FABP-3 and FABP-7 (Yan et al. 2018, compound 4j). We administered SBFI-103 locally into the prelimbic region (PLC) of the mPFC, a cortical region that expresses FABP-5 (Shimamoto et al. 2014) and is a strong top-down modulator of contextual fear and anxiety (Kim et al. 2013), and performed anxiety, fear memory expression, and cognitive tests in rats. Furthermore, in order to investigate the potential neuronal and molecular mechanisms underlying the effects of FABP-5 inhibition, we challenged the effects of SBFI-103 with CB1R, CB2R, GPR55, and PPAR γ antagonists. Finally, using *in vivo* electrophysiology in anesthetized rats, we examined the neuronal firing and oscillatory activity patterns in 2 functionally interconnected pathways within the PLC; the BLA and ventral hippocampus (VHipp) following SBFI-103 exposure.

Materials and methods

Animals

Male Sprague Dawley rats (300–350 g, 8–10 weeks old; Charles River Laboratories, Quebec, Canada) were pair-housed until surgeries and single-housed afterwards. Animals were kept in a temperature (22 ± 2 °C), humidity ($55 \pm 10\%$), and light (light on from 7 AM to 7 PM) controlled room with food and water available *ad libitum*. Behavioral tests were conducted between 9 AM and 5 PM. All procedures were performed in accordance

with the Canadian Council of Animal Care and the Animal Care Committee at the University of Western Ontario, Ontario.

Surgical procedures

Rats were anesthetized with a ketamine (80 mg/kg, Vetoquinol)–xylazine (6 mg/kg, Bayer) mixture, administered intraperitoneally (*i.p.*). Animals were placed in a stereotaxic device (Kopf), and stainless steel guide cannulae (22 gauge) were bilaterally implanted into the PLC (3.2 mm anterior, 1.8 mm lateral (15° angle), 3 mm ventral from Bregma, (Paxinos and Watson 2013). Cannulae were secured using screws and dental acrylic cement. To reduce pain and inflammation, animals received Meloxicam (1 mg/kg, *s.c.*, Boehringer Ingelheim) immediately before and 1 day after surgery. Behavioral tests started after a 1-week recovery period with daily inspection of recovery status.

Drugs

SBFI-103 (9-Fluorenylmethyl *a*-3-hydroxycarbonyl-2, 4-di(2-methoxyphenyl)-cyclobutane-1-carboxylate), a selective inhibitor of FABP-5 with negligible affinity for FABP-3 and FABP-7, was synthesized as previously described (Yan et al. 2018). SBFI-103 was administered in 2 doses (0.5 or 5 $\mu\text{g}/\text{side}$). Other drugs (Cayman Chemical): CB1R inverse agonist SR141716 (rimonabant; 0.5 $\mu\text{g}/\text{side}$), CB2R inverse agonist AM630 (5 $\mu\text{g}/\text{side}$), GPR55 antagonist CID16020046 (1 $\mu\text{g}/\text{side}$), and PPAR γ antagonist T0070907 (0.2 $\mu\text{g}/\text{side}$) were co-administered with 5 μg SBFI-103 or vehicle. The doses of the drugs were determined by our pilot studies and previous studies in the literature, and are inversely proportional to the K_i values of their respective target receptors (Zhang et al. 2014; Loureiro et al. 2016; Kramar et al. 2017). All drugs were dissolved in saline containing 10% DMSO–5% Cremophor and infused bilaterally (volume: 0.5 $\mu\text{L}/\text{side}$, rate of infusion: 0.5 $\mu\text{L}/\text{min}$) using a 10 μL Hamilton syringe with Polymicro capillary tubing protruding 1 mm beyond the implanted guide cannula. Each behavioral test commenced 5 min after the micro-infusions.

Behavioral tests

Light–dark box

The test arena consisted of 2 identical-sized compartments (50 × 25 × 37 cm), which were divided by a wall with a 10 × 10 cm door. One compartment was fully dark, while the other was illuminated with an overhead lamp. Rats were placed in the light chamber with their heads facing the wall opposite to the door, and their activities were recorded for 10 min, as previously described (De Felice et al. 2021). Time spent in the light chamber, number of transitions and latency to enter the light chamber for the first time were analyzed manually to assess the anxiety-like behavior.

Elevated plus maze

The apparatus consisted of 4 arms (10 × 50 cm), raised 50 cm above the floor. Two opposite arms were enclosed with walls (40 cm), while the other 2 arms were open. Rats were placed in the center of the apparatus, facing the closed arm, and their activities were recorded for 10 min, as previously described (Szkudlarek et al. 2019). % time spent in the open arm ((open arm time/open arm + closed arm time) * 100) and % open arm entries ((open arm entry/open arm + closed arm entry) * 100) were analyzed manually to assess the anxiety-like behavior.

Open field

Rats were placed in an automated open field (OF) arena (40 × 40 × 40 cm; San Diego Instruments, San Diego, CA, USA), where locomotor activity and rearing were recorded and analyzed automatically for 30 min, as previously described (Kramar et al. 2017).

Contextual fear conditioning

Two distinct test environments were used for fear acquisition and retrieval (Fig. 2A). On day 1, animals received 2 5-min acquisition sessions (>3 h apart) in environment A, during which they received 3 foot-shocks (2 s, 0.9 mA) at pseudorandomized interval. On day 2, animals received micro-infusions and 5 min later were placed in environment B (neutral environment) for 5 min to test fear generalization. Immediately afterwards, animals were transferred to environment A (shock environment) to test contextual fear memory retrieval. On day 15, animals were placed again in environment A for 5 min to test remote fear memory retrieval. The percent time animal spent freezing in each condition was analyzed manually to assess the expression of fear. Freezing was defined as the absence of movement aside of respiration.

Spontaneous alternation

The test apparatus consisted of a Y-shaped maze with three identical arms (length: 50 cm, height: 40 cm). Rats were placed in the center of the arm and their activities were recorded for 10 min, as previously described (Szkudlarek et al. 2019). An arm entry was scored only when all 4 paws of the animal were in that arm. The total number of arm entries and spontaneous alternation (SA) % were assessed. A SA occurs when the rat enters a different arm in 3 consecutive arm entries.

Temporal order object recognition

The test arena consisted of an 80 × 80 × 50 cm box. The test session consisted of 3 4-min trials with an inter-trial interval (ITI) of 60 min, during which animals were allowed to explore 2 objects (acquisition 1: objects AA; acquisition 2: objects BB; test phase; objects AB). Object exploration was considered when the animal was sniffing the object.

Prepulse inhibition of the startle reflex

Prepulse inhibition (PPI) testing was performed as previously described (De Felice et al. 2021). Animals were confined within transparent tubes (25 × 12 cm), placed on a movement-sensitive platform in an enclosed sound-attenuating box (Panlab). On day 1, animals were acclimated to the startle box (5 min, 65 dB background noise). On day 2, animals were tested with an input/output function, consisting of 11 ascending startle pulses (white noise, from 65 to 115 dB, 5 dB increment, 20 ms duration, 1 min ITI). On day 3, PPI test was performed, during which animals received the following pseudorandomized trials (7 conditions, 10 trials each, 15–20 s ITI): pulse alone (110 dB), pulse + prepulse (72, 76, or 80 dB) using 2 different interstimulus intervals (30 or 100 ms). The %PPI was calculated with the formula of: %PPI = 100 – [100 × (startle amplitude of prepulse + pulse trials/startle amplitude of pulse alone trials)].

Histology

Following the completion of behavioral experiments, rats were sacrificed using sodium pentobarbital (Euthanyl). Brains were removed and stored at –80 °C until slicing. 100 μm thick coronal sections were cut, mounted on glass slides, stained with cresyl violet, and examined under a light microscope for the verification of cannula placements within the PLC region (Fig. 1A).

In vivo electrophysiology

In vivo extracellular recordings in the BLA, VHipp, nucleus accumbens shell (NAccSh), and ventral tegmental area (VTA) were performed as described previously (Renard et al. 2017; De Felice et al. 2021). Naïve rats were anesthetized with urethane (1.4 g/kg, i.p.) and placed in a stereotaxic apparatus (Kopf). The rat's body temperature was maintained at 37 °C (±1°) using a rectal temperature controller. The skull was exposed and according to the rat brain atlas (Paxinos and Watson 2013), craniotomies were performed above the target areas (in mm from Bregma: infusion site: mPFC: 10° anterior angle, 3.8 anterior, 0.8 lateral; recording sites: BLA: 2.4–2.7 posterior, 4.8–5 lateral; VHipp: 5.6–5.8 posterior, 5.8–6 lateral; NAccSh: 1.8–2.2 anterior, 0.7–0.9 lateral; VTA: 5–5.2 posterior, 0.8–1 lateral). Intra-PLC infusions were performed using an injection cannula connected to a 10 μL Hamilton syringe with Polymicro capillary tubing (3.1 mm ventral from dura). Extracellular recordings were performed in target regions (depth in mm from dura: BLA: 6.5–8; VHipp: 4–6; NAccSh: 5.5–7; VTA: 7–9) using glass microelectrodes (impedance: 8 ± 2 MΩ) filled with 2% pontamine sky blue solution (Sigma-Aldrich). Extracellular signals were filtered (bandpass, 0.3–5 kHz), amplified (Multiclamp 700B amplifier, Molecular Devices), digitized at 25 kHz, and recorded (Digidata 1440A System and pClamp Software, Molecular Devices). Neurons in each region were identified using previously established criteria (Renard et al. 2017; Norris et al. 2019; De Felice et al. 2021),

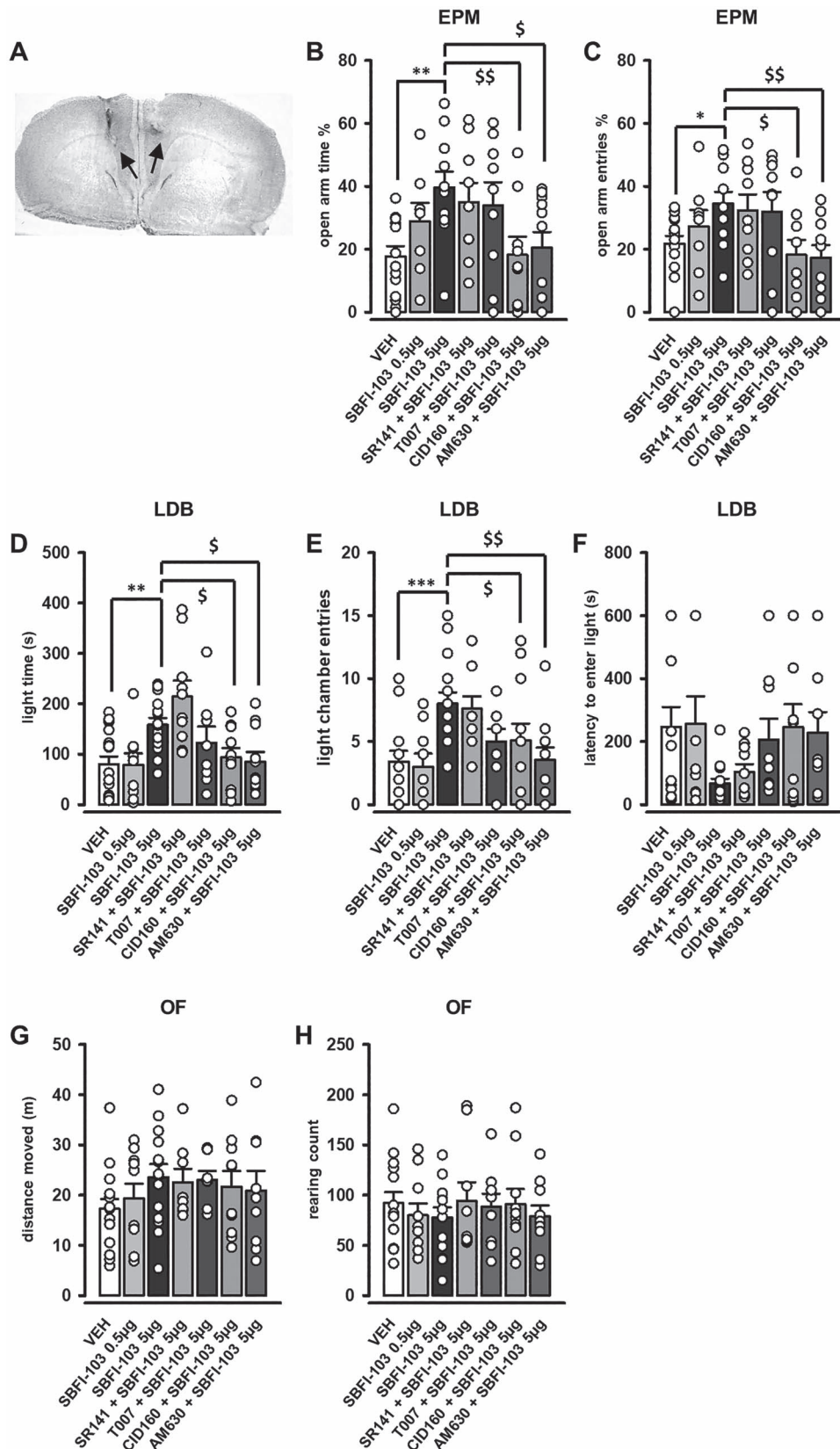


Fig. 1. Acute intra-PLC SBFI-103 administration induces anxiolytic-like behavior, which is prevented by AM630 or CID160 co-administration. (A) Microphotograph of representative cannula placement within the PLC. Arrows show the tip of injector cannula. (B and C) 5 µg/hemisphere intra-PLC SBFI-103 infusion increases time spent in the open arm (B) and open arm entries (C) in the EPM. These elevations are reversed by AM630 or CID160 co-administration. Open arm time % = 100 * open arm time / open + closed arm time. Open arm entries % = 100 * open arm entries / open + closed arm entries. (D and E) 5 µg/hemisphere intra-PLC SBFI-103 infusion increases time spent in the light chamber (D) and light chamber entries (E) in the LDB. These elevations are reversed by AM630 or CID160 co-administration. (F) 5 µg/hemisphere intra-PLC SBFI-103 infusion did not alter latency to enter light chamber in the LDB. (G and H) 5 µg/hemisphere intra-PLC SBFI-103 infusion did not alter locomotion (G) or rearing (H) in the OF. Data represent mean ± SEM. EPM: N = 71 (8–14 per group) LDB: N = 82 (8–17 per group) OF: N = 76 (8–16 per group). Groups were compared using 1-way ANOVA followed with Fisher’s LSD post hoc test. *P < 0.05, **P < 0.01, ***P < 0.001 compared to VEH. \$P < 0.05, \$\$P < 0.01, \$\$\$P < 0.001 compared to 5 µg/hemisphere SBFI-103.

isolated, and recorded for at least 36 min (5 min baseline + 1 min infusion + 30 min postinfusion). Local field potential (LFP) signals were downsampled to 1 kHz, lowpass filtered (IIR Butterworth filter at 170 Hz, filter order: 3), and the power of oscillations between 0 and 58 Hz was calculated using a spectrogram function of NeuroExplorer (NexTechnologies). The spike rate and oscillatory activities were normalized to the baseline activity, and postinfusion activities were calculated as % change from baseline. For histological analyses, recording electrode positions were marked with an iontophoretic deposit of pontamine sky blue (−20 mA, 15 min) followed with histological procedures as previously described (Renard et al. 2017).

Data analysis

Data are presented as mean + SEM and were analyzed using 2-tailed t-tests, 1-way or 2-way ANOVA where appropriate (Sigma Plot). Post hoc analyses were calculated using Fisher's LSD. Kruskal–Wallis H test was used for nonparametric datasets, followed by Mann–Whitney U tests between relevant groups. Behavioral activities other than OF and PPI were recorded and analyzed later manually using Behavior software (www.pmbogusz.net). The significance level was set to $P < 0.05$.

Results

Intra-PLC FABP-5 inhibition reduces anxiety-like behavior through CB2R- and GPR55-dependent mechanisms

Given previous evidence demonstrating that elevated eCB neurotransmission induces anxiolytic effects in rodents (Kathuria et al. 2003; Gunduz-Cinar, MacPherson, et al. 2013a), we hypothesized that FABP-5 inhibition within the PLC may produce anxiolytic behavioral effects. The effects of FABP-5 inhibition by SBFI-103 were later challenged with CB1R, CB2R, GPR55, and/or PPAR γ antagonists using SR141716, AM630, CID160, and T007, respectively. Anxiety behaviors were assessed using the elevated plus maze (EPM) and light–dark box (LDB) tests. One-way ANOVA revealed a treatment effect in open arm time ($F_{(6,64)} = 2.945$, $P = 0.013$) and open arm entries ($F_{(6,64)} = 2.729$, $P = 0.02$) in the EPM test as well as light chamber time ($F_{(6,75)} = 5.839$, $P < 0.001$) and light chamber entries ($F_{(6,75)} = 4.121$, $P = 0.001$) in the LDB test. Post hoc analyses showed that SBFI-103 infusion was dose-dependently anxiolytic as animals receiving 5 $\mu\text{g}/\text{hemisphere}$ SBFI-103 spent more time in the open arm ($P = 0.002$; Fig. 1B), entered it more frequently ($P = 0.025$; Fig. 1C), spent more time in the light chamber ($P = 0.003$; Fig. 1D) and entered it more frequently ($P < 0.001$, Fig. 1E) compared to the control animals; however, these effects were absent when the animals received 0.5 $\mu\text{g}/\text{hemisphere}$ SBFI-103 ($P_s > 0.05$). Interestingly, SBFI-103-induced anxiolytic effects in the EPM and LDB were prevented by co-administration

of AM630 and CID160 (open arm time: $P = 0.011$ and $P = 0.007$; open arm entries: $P = 0.005$ and $P = 0.011$; light time: $P = 0.011$ and $P = 0.021$; light entries: $P = 0.002$ and $P = 0.035$, respectively), but not by SR141716 or T007 ($P_s > 0.05$). While the data showed a trend in SBFI-103-induced decrease in latency to enter the light chamber (Fig. 1F), 1-way ANOVA was not significant ($F_{(6,75)} = 1.694$, $P = 0.134$). There was no treatment effect when SR141716, AM630, CID160, or T007 was administered alone (open arm time: $F_{(4,40)} = 0.777$; open arm entries: $F_{(4,40)} = 0.436$, light time: $F_{(4,47)} = 0.313$, light entries: $F_{(4,47)} = 0.722$; latency to enter light: $F_{(4,47)} = 1.834$; $P_s > 0.05$; Supplementary Fig. S1A–E). These results indicate that intra-PLC FABP-5 inhibition results in a dose-dependent anxiolytic behavioral phenotype, which is dependent on CB2R- and GPR55-mediated mechanisms. Interestingly, CB1R-mediated mechanisms do not appear to be involved in these effects.

Intra-PLC FABP-5 inhibition does not alter locomotor activity

Pharmacological agents modulating eCB signaling may induce locomotion alterations (Renard et al. 2017), which could underlie or influence FABP-5 inhibitor-induced anxiolysis. The results showed that neither FABP-5 inhibition nor co-application of SBFI-103 with CB1R, CB2R, GPR55, and PPAR γ antagonists affected locomotion ($F_{(6,69)} = 0.837$, $P > 0.05$) or rearing ($F_{(6,69)} = 0.308$, $P > 0.05$; Fig. 1G and H). When SR141716, AM630, CID160, or T007 was administered alone, a treatment effect was again not detected (locomotion: $F_{(4,39)} = 0.788$; rearing: $F_{(4,38)} = 0.855$, $P_s > 0.05$; Supplementary Fig. S1F and G).

Intra-PLC FABP-5 inhibition reduces contextual fear expression through CB1R- and CB2R-dependent mechanisms

In order to investigate the effects of intra-PLC FABP-5 inhibition on fear memory expression (Kim et al. 2013), we designed a protocol that was adapted from Poulos et al. (2016). As shown in Fig. 2A, 24 h after contextual fear memory acquisition, freezing responses of the animals were measured in a novel environment (fear generalization) and in the previously experienced fear environment (contextual fear retention). Two-way repeated measures ANOVA revealed a significant treatment \times environment interaction ($F_{(5,46)} = 3.378$, $P = 0.011$). Post hoc analyses showed that SBFI-103 infusion reduced contextual fear ($P = 0.025$; Fig. 2B), and this effect was reversed by co-administration of SR141716 ($P = 0.025$) and AM630 ($P = 0.024$), and partially reversed by co-administration of CID160 ($P = 0.06$), but not by T007 ($P > 0.05$). Surprisingly, despite SBFI-103 infusion having no effect on fear generalization ($P > 0.05$), SR141716 co-infused animals showed elevated freezing (vs. VEH: $P = 0.012$; vs. SBFI-103: $P = 0.019$), suggesting exacerbated fear generalization by SR141716. These findings demonstrate that intra-PLC

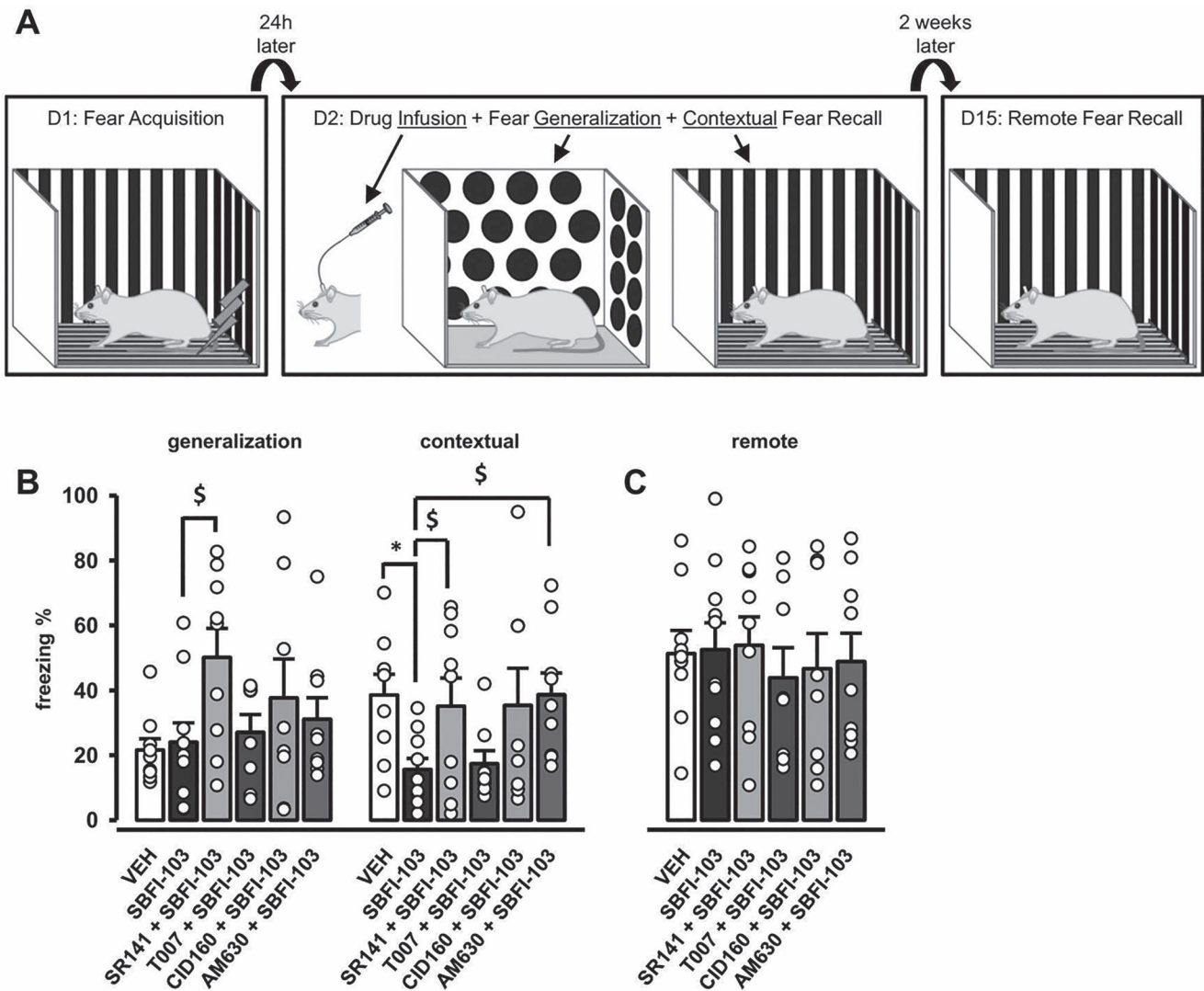


Fig. 2. Intra-PLC SBFI-103 administration before fear retrieval reduces contextual fear expression, which is prevented by AM630 or SR141716 co-administration. (A) Schematic representation of the fear conditioning procedure. Environment A ($30 \times 30 \times 60$ cm white Plexiglas box with black stripes and a metallic floor grid) was cleaned and odored with 70% ethanol and environment B ($30 \times 30 \times 60$ cm white Plexiglas box with black circles and a smooth Plexiglas floor) with 0.5% acetic acid. Fear acquisition took place in environment A. A day later, effects of intra-PLC SBFI-103 administration on fear generalization (environment B) and contextual fear expression (environment A) were assessed using freezing response. 14 days later, remote fear response was assessed (no infusion before test). (B) $5 \mu\text{g}/\text{hemisphere}$ intra-PLC SBFI-103 infusion attenuated expression of contextual fear but did not influence expression of generalized fear. Attenuated contextual fear was reversed by AM630 or SR141716 co-infusion. SR141716 co-infusion also increased generalized fear expression. (C) $5 \mu\text{g}/\text{hemisphere}$ intra-PLC SBFI-103 infusion before fear expression (day 2) did not alter fear memories, as tested by remote fear recall (environment A) on day 15. Freezing was defined as the absence of movement aside of respiration. Data represent mean \pm SEM. $N = 52$ (8–10 per group). Groups were compared using 2-way repeated measures ANOVA (B) or 1-way ANOVA (C) followed with Fisher's LSD post hoc test. * $P < 0.05$ compared to VEH. $^{\$}P < 0.05$ compared to $5 \mu\text{g}/\text{hemisphere}$ SBFI-103.

FABP-5 inhibition attenuates contextual fear expression through CB1R- and CB2R-mediated mechanisms. Furthermore, CB1R modulates generalization of fear without the involvement of FABP-5.

To test whether the SBFI-103-induced reduction of contextual fear was persistent, we re-tested contextual fear responses 2 weeks after the initial fear retention test without re-infusing drugs. One-way ANOVA revealed no treatment effect on remote fear recall ($F_{(5,46)} = 0.268$, $P > 0.05$, Fig. 2C), suggesting that infusions before the initial fear retention test had no impact on long term fear memory processing.

Intra-PLC FABP-5 inhibition does not influence memory performance or sensorimotor gating

FABP-5 has been reported to regulate cognitive function as genetic ablation of FABP-5 impairs spatial learning and memory (Yu et al. 2014). Therefore, we investigated the effects of intra-PLC FABP-5 inhibition on spatial working memory and short-intermediate term temporal recognition memory (TRM) using SA and temporal-order object recognition (TOR) tests, respectively. A 2-tailed t test revealed no effect of SBFI-103 ($t_{11} = 0.715$, $P > 0.05$) on alternation performance in SA (Fig. 3A). Furthermore, number of alternations remained

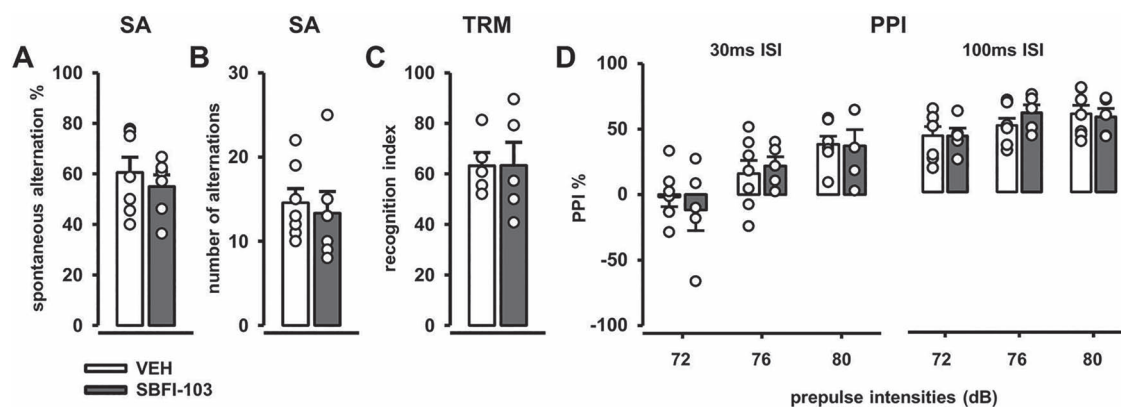


Fig. 3. Acute intra-PLC SBFI-103 administration does not influence cognitive performance or sensorimotor gating. (A, B) 5 μ g/hemisphere intra-PLC SBFI-103 infusion did not alter SA performance (A) or number of alternations (B) in the Y-maze. A SA occurs when the rat enters a different arm in 3 consecutive arm entries. SA % = 100 * number of SAs/(total number of arm entries-2). (C) 5 μ g/hemisphere intra-PLC SBFI-103 infusion did not alter TRM performance. Recognition index = 100 * time spent exploring less recently encountered object/time spent exploring both objects. (D) 5 μ g/hemisphere intra-PLC SBFI-103 infusion did not alter PPI with either ISI used (30 and 100 ms). %PPI = 100 - [100 * (startle amplitude of prepulse + pulse trials/startle amplitude of pulse alone trials)]. Data represent mean + SEM. SA: N = 13 (6-7 per group) TRM: N = 10 (5 per group) PPI: N = 12 (5-7 per group). Groups were compared using t-test (A-C) or 2-way repeated measures ANOVA (D).

intact ($t_{11} = 0.416$, $P > 0.05$; Fig. 3B), providing further support for the absence of locomotor-altering effects of SBFI-103. Similarly, analysis of TOR test revealed no effect of SBFI-103 on the recall of recognition memory performance ($t_8 = -0.0136$, $P > 0.05$; Fig. 3C). Thus, an effective anxiolytic dose of the intra-PLC FABP-5 inhibitor appears to produce no side effects on working memory or recognition memory recall.

To test whether FABP-5 inhibition alters reactivity to sensory stimuli, we examined the effects of intra-PLC SBFI-103 on PPI. Two-way repeated measures ANOVA revealed a significant effect of prepulse intensity (30 ms interstimulus-interval [ISI]: $F_{(2,20)} = 21.192$, $P < 0.001$, 100 ms ISI: $F_{(2,20)} = 13.73$, $P < 0.001$); however, a treatment effect was not detected (30 ms ISI: $F_{(1,10)} = 0.0241$, 100 ms ISI: $F_{(1,10)} = 0.0804$, $P_s > 0.05$) (Fig. 3D). Thus, sensorimotor gating system remains intact after intra-mPFC FABP-5 inhibition.

Intra-PLC FABP-5 inhibition attenuates firing of BLA putative pyramidal neurons in a CB2R-dependent manner

The PLC region modulates emotional behavior by exerting top-down control over BLA neuronal activity. Thereafter, long-range BLA projections to PLC and vHipp control the expression of emotions, most notably fear and anxiety (McGarry and Carter 2017). Bidirectional functional connections between mPFC and BLA, which are modulated by eCB signaling, controls emotional learning plasticity, and memory formation (Laviolette and Grace 2006; Tan et al. 2011). Given our behavioral results indicating decreased expression of fear and anxiety-like behaviors by intra-PLC FABP-5 inhibition, we hypothesized that FABP-5-inhibitor-induced behavioral effects may be associated with attenuated activation of projection neurons in the BLA. After isolating a total of 45 pyramidal neurons in the BLA, we analyzed their spiking activity pre- and post-intra-PLC infusions of

VEH, SBFI-103, and a combination of the CB2 antagonist AM630 + SBFI-103 using in vivo electrophysiological recordings. The effects of the infused agents were analyzed as 3 10-min bins (Fig. 4B) and as 30 min overall activity (Fig. 4C), with example recording traces shown in Fig. 4A and histograms shown in Fig. 4E. Two-way repeated measures ANOVA revealed a robust effect of treatment ($F_{(2,42)} = 7.897$, $P = 0.004$). Post hoc comparisons revealed SBFI-103-induced attenuation of firing rate at 10–20 min ($P = 0.006$) and 20–30 min ($P = 0.003$) postinfusion (Fig. 4B). Furthermore, SBFI-103 infusion caused a 30.7% reduction of overall firing rate ($P = 0.009$; Fig. 4C). AM630 co-administration prevented SBFI-103-induced attenuation of spiking at 10–20 min ($P = 0.002$) and 20–30 min ($P = 0.043$) postinfusions and in overall activity (13.6% increase; $P = 0.005$). Population analysis of BLA neurons demonstrated that 68.8% (11/16) of BLA neurons showed decreased activity following SBFI-103 infusion, whereas 23.5% (4/17) showed decreased activity after VEH infusion and 16.7% (2/12) after AM630 + SBFI-103 co-infusion (Fig. 4D). Altogether, consistent with our behavioral findings, these data demonstrate a CB2R-dependent attenuation of BLA neuronal transmission by intra-PLC FABP-5 inhibition, which possibly underlies FABP-5 inhibition-induced changes in the expression of fear and anxiety, as suggested by our behavioral pharmacological challenge studies.

Intra-PLC FABP-5 inhibition elevates firing of vHipp putative pyramidal neurons in a CB2R-dependent manner

Given that the firing activities of pyramidal BLA neurons are attenuated by intra-PLC FABP-5 inhibition and that BLA to vHipp inputs modulate anxiety-like behavior (Felix-Ortiz et al. 2013), we isolated a total of 34 pyramidal neurons in the CA1 region of the vHipp and analyzed their firing frequencies pre- and post-intra-PLC infusions of VEH, SBFI-103, and AM630 + SBFI-103. The effects

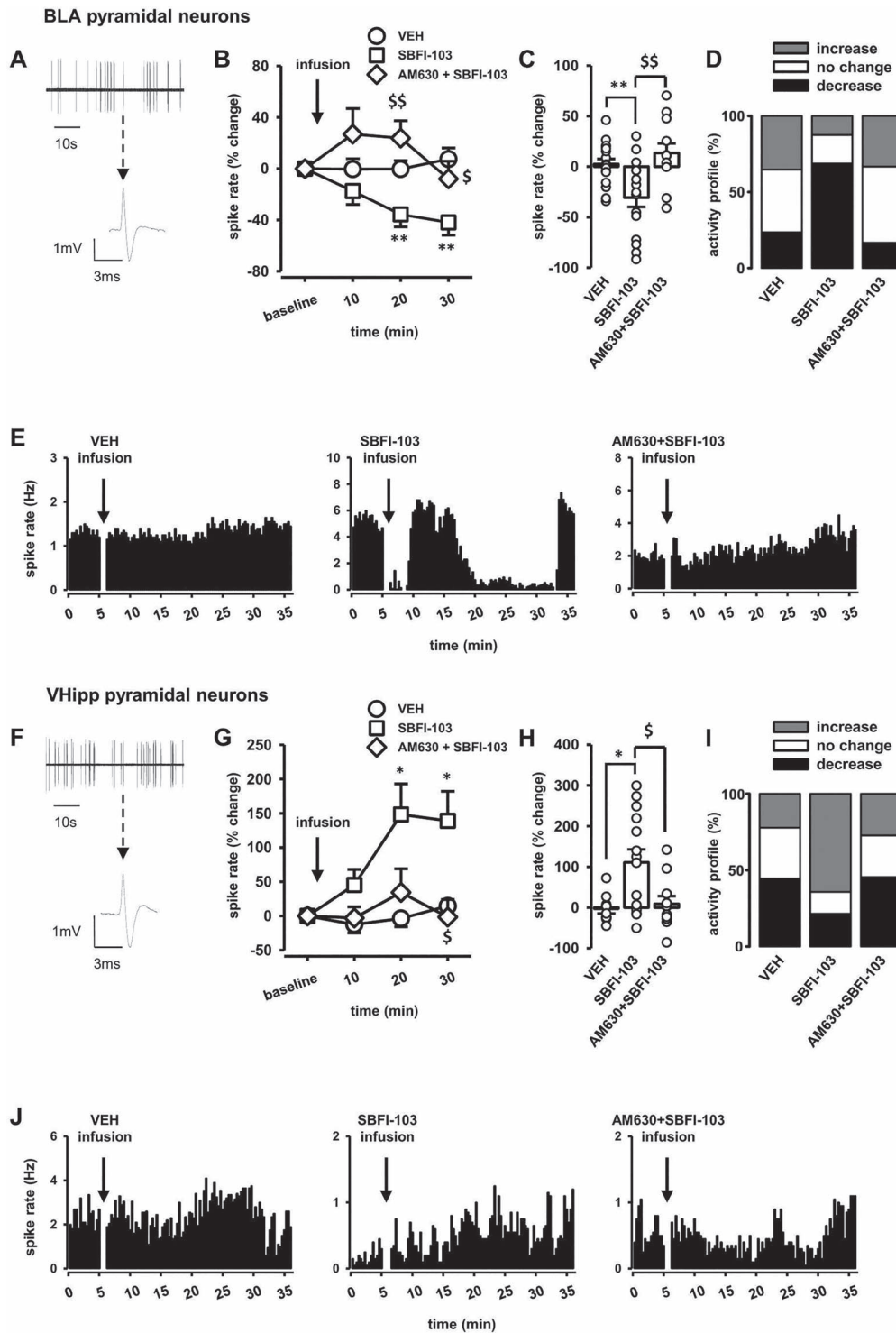


Fig. 4. Intra-PLC SBFI-103 administration attenuates firing of BLA putative principal neurons and elevates firing of VHipp putative pyramidal neurons, both of which are prevented by AM630 co-administration. (A) Representative example showing spiking activity of a BLA pyramidal neuron (top) and a single spike (bottom). (B, C) 5 μ g intra-PLC SBFI-103 infusion reduced the spiking rate of BLA neurons, as shown in 10 min bins (B) and as overall 30 min postinfusion activity (C). Attenuated firing rate was restored by AM630 co-infusion. Data are represented as % change from baseline. (D) Percentage of BLA neurons showing relative changes in firing rates (increase, decrease, or no change) after the infusion of vehicle, SBFI-103 and AM630 + SBFI-103. A neuron was considered to change its firing rate if the difference in firing rate between pre- and post-infusion is >10%. (E) Sample histograms (20 s bins) of BLA neurons pre- and post-infusion of vehicle (left panel), SBFI-103 (middle panel), and AM630 + SBFI-103 (right panel). (F) Representative example showing spiking activity of a VHipp pyramidal neuron (top) and a single spike (bottom). (G, H) 5 μ g intra-PLC SBFI-103 infusion increased the spiking rate of VHipp neurons, as shown in 10 min bins (G) and as overall 30 min postinfusion activity (H). Elevated firing rate was restored by AM630 co-infusion. Data are represented as % change from baseline. (I) Percentage of VHipp neurons showing relative changes in firing rates (increase, decrease, or no change) after the infusion of vehicle, SBFI-103 and AM630 + SBFI-103. A neuron was considered to change its firing rate if the difference in firing rate between pre- and post-infusion is >10%. (J) Sample histograms (20 s bins) of VHipp neurons pre- and post-infusion of vehicle (left panel), SBFI-103 (middle panel), and AM630 + SBFI-103 (right panel). Data represent mean \pm SEM. BLA: N = 45 neurons (12–17 per group) VHipp: N = 34 neurons (9–14 per group). Non-normally distributed datasets were compared using Kruskal–Wallis test followed with Mann–Whitney U tests between the relevant groups. *P < 0.05, **P < 0.01 compared to VEH. \$P < 0.05, \$\$P < 0.01 compared to SBFI-103.

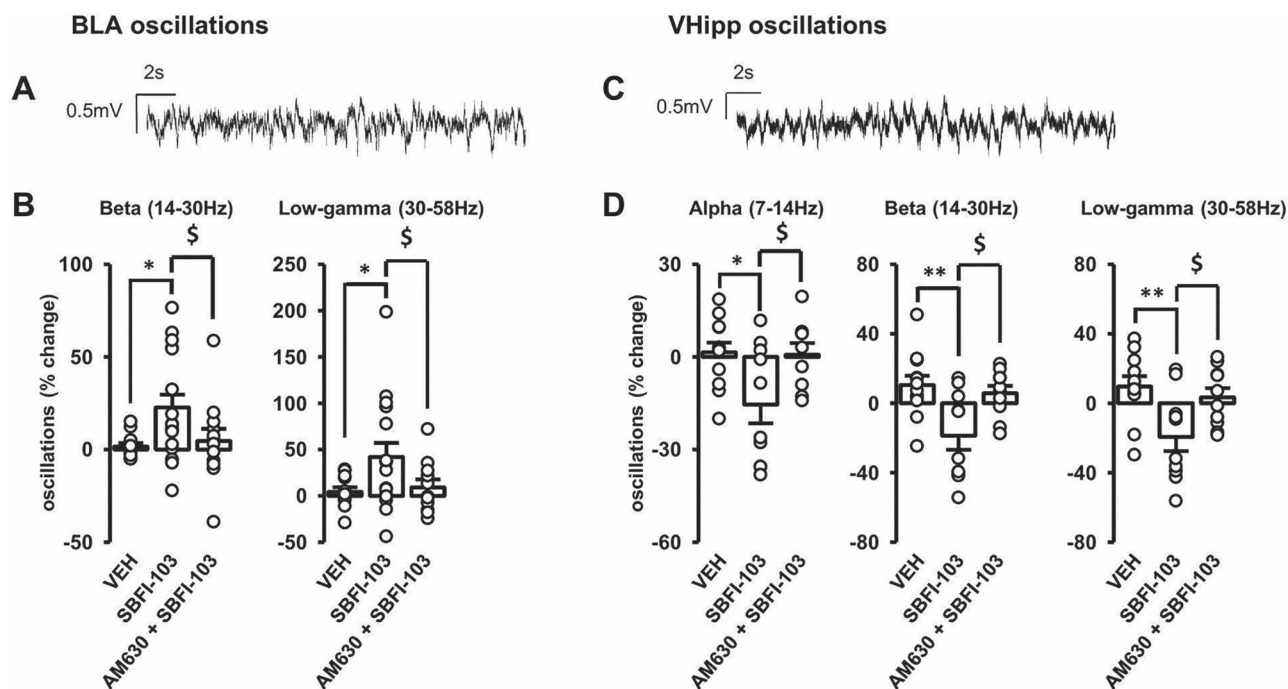


Fig. 5. Intra-PLC SBFI-103 administration (5 μ g) elevates the power of beta and low-gamma oscillations in the BLA and attenuates the power of alpha, beta, and low-gamma oscillations in the VHipp, all of which are prevented by AM630 co-administration. (A) Example recording traces of BLA oscillations. (B) Group summaries showing increased power of beta (left panel) and low-gamma (right panel) oscillations in the BLA following SBFI-103 administration. Elevations were restored by AM630 co-administration. Data are represented as % change (average of 30 min postinfusion) from baseline. (C) Example recording traces of VHipp oscillations. (D) Group summaries showing decreased power of alpha (left panel), beta (middle panel), and low-gamma (right panel) oscillations in the VHipp following SBFI-103 administration. Reductions were restored by AM630 co-administration. Data are represented as % change (average of 30 min postinfusion) from baseline. BLA: $N = 41$ recordings (10–17 per group) VHipp: $N = 32$ recordings (9–12 per group). Groups were compared using 1-way ANOVA followed with Fisher's LSD post hoc test. * $P < 0.05$, ** $P < 0.01$ compared to VEH. $^{\$}P < 0.05$ compared to SBFI-103.

of the infused agents were analyzed as 3 10-min bins (Fig. 4G) and as 30 min overall activity (Fig. 4H), with example recording traces shown in Fig. 4F and histograms shown in Fig. 4J. Two-way repeated measures ANOVA revealed a significant effect of treatment ($F_{(2,31)} = 6.173$, $P = 0.028$) and time ($F_{(2,59)} = 3.812$, $P = 0.028$). Post hoc comparisons demonstrated SBFI-103-induced enhancement of firing rate at 10–20 min ($P = 0.025$) and 20–30 min ($P = 0.05$) postinfusion (Fig. 4G). Furthermore, SBFI-103 infusion caused a 110.9% elevation of overall firing rate ($P = 0.021$; Fig. 4H). AM630 co-administration counteracted SBFI-103-induced elevation of firing rate at 20–30 min ($P = 0.015$) postinfusion and restored overall activity (9.1% increase; $P = 0.035$). Population analysis of VHipp neurons revealed that 64.3% (9/14) of VHipp neurons showed elevated activity after SBFI-103 infusions, whereas 22.2% (2/9) showed elevated activity after VEH infusion and 27.3% (3/11) after AM630 + SBFI-103 co-infusion (Fig. 4I). Intra-PLC FABP-5 inhibition, however, did not affect neuronal firing in the NAccSh (Supplementary Fig. S2A–C) or VTA (Supplementary Fig. S2D–F). These results indicate that intra-PLC FABP-5 inhibition significantly increases activity of putative VHipp pyramidal neurons, which is prevented by CB2R antagonism. Furthermore, intra-PLC SBFI-103 does not modulate mesolimbic dopamine activity states, suggesting FABP-5 inhibition to pose a low risk of addictive liability.

Intra-PLC FABP-5 inhibition alters the power of local field potentials in the BLA and VHipp in a CB2R-dependent manner

In order to investigate the effects of intra-mPFC FABP-5 inhibition on LFP in the BLA and VHipp, LFPs were recorded concurrently with single-unit activities. The powers of delta (0.5–4 Hz), theta (4–7 Hz), alpha (7–14 Hz), beta (14–30 Hz), and low-gamma (30–58 Hz) oscillations were analyzed pre- and post-infusions of VEH, SBFI-103, and AM630 + SBFI-103. Effects of the infused agents were analyzed for 30 min, with example recording traces shown for BLA (Fig. 5A) and VHipp (Fig. 5C). In the BLA, 1-way ANOVA revealed significant treatment effects for beta ($F_{(2,38)} = 3.793$, $P = 0.031$) and low-gamma oscillations ($F_{(2,35)} = 3.832$, $P = 0.031$), but not for other bands ($P_s > 0.05$, data not shown). Post hoc comparisons demonstrated SBFI-103-induced enhancements in the power of beta ($P = 0.018$) and low-gamma ($P = 0.025$) oscillations, both of which were prevented by AM-630 co-administration (beta: $P = 0.04$, low-gamma: $P = 0.027$; Fig. 5B). In the VHipp, 1-way ANOVA revealed significant treatment effects for alpha ($F_{(2,28)} = 4.611$, $P = 0.019$), beta ($F_{(2,29)} = 6.575$, $P = 0.004$) and low-gamma oscillations ($F_{(2,28)} = 5.41$, $P = 0.01$), but not for other bands ($P_s > 0.05$, data not shown). Post hoc comparisons demonstrated SBFI-103-induced attenuations in the power of alpha ($P = 0.01$), beta ($P = 0.002$), and low-gamma ($P = 0.004$) oscillations, all of which were prevented by AM-630

co-administration (alpha: $P=0.02$ beta: $P=0.01$, low-gamma: $P=0.022$; Fig. 5D).

Discussion

Fatty acids not only are effective energy sources, but also act as signaling molecules causing numerous physiological effects in the brain. Since eCB signaling is involved with the regulation of emotions, and alterations in eCB signaling within the corticolimbic system are associated with neuropsychiatric conditions including anxiety disorders, it serves as a promising target for novel anxiolytic pharmacotherapies. Our behavioral findings indicate that intra-PLC FABP-5 inhibition reduces anxiety-like behaviors and the expression of contextual fear without affecting locomotor activity, learning, memory performance, or sensorimotor gating. Furthermore, our electrophysiological findings suggest that intra-PLC FABP-5 inhibition does not influence the dopaminergic signaling pathways, which might make it safer than widely prescribed anti-anxiety medications in terms of addictive liability. The present findings identify a promising role for FABP-5 inhibition as a novel anxiolytic pharmacotherapy as well as a novel CB2R-dependent FABP-5 signaling pathway in the mPFC, which modulates anxiety and fear expression.

The observed behavioral effects in this study are potentially due to elevated AEA-mediated neurotransmission as FABP-5 promotes cellular uptake and hydrolysis of AEA and AEA levels are known to be importantly involved in affective regulation. Indeed, AEA quantification studies using tandem liquid chromatography-mass spectrometry have found elevated cerebral AEA levels after pharmacological inhibition and/or genetic ablation of FABP-5 (Kaczocha et al. 2014; Yu et al. 2014). FABP-5 inhibition, however, did not alter cerebral 2-AG levels or the activity of FAAH (Kaczocha et al. 2014), suggesting that our findings are not likely mediated via these mechanisms. As an alternative mechanism, FABP-5 inhibition-induced anxiolytic effects might be mediated by other N-acyl ethanolamines palmitoylethanolamide (PEA) and oleoylethanolamide (OEA). For example, pharmacological inhibition of FABP-5/7 by intracerebroventricular infusion of SBFI-26, as well as genetic ablation of FABP-5/7, elevated PEA and OEA levels in mice brain (Kaczocha et al. 2015; Peng et al. 2017). Given the role of PEA in the regulation of fear and anxiety behaviors (Locci and Pinna 2019), elevated PEA might also be involved in modulating FABP-5 inhibition-induced anxiolytic-like behavioral effects. Future studies are required to more clearly define these underlying mechanisms.

Tissue-specific expression patterns of FABPs and region-specific expression patterns of FABP-5 in adult brain make it a particularly promising target for pharmacotherapeutic interventions. This advantage of FABPs should significantly decrease the likelihood of off-target side effects when administered systemically.

Indeed, current anxiolytic treatments are associated with significant deleterious side-effects, including dependence, withdrawal, and cognitive impairments (Griebel and Holmes 2013), which are major therapeutic limitations. While lower rates of adverse side-effects have been observed with FAAH inhibitors (Li et al. 2012), the wide expression of FAAH throughout the body potentially makes targeting FABP-5 safer and more tolerable. For example, systemic inhibition of FAAH was linked with hyperglycemia and insulin resistance due to high levels of FAAH expression in the liver (Tourño et al. 2010). Systemic inhibition of FABP-5 and FABP-7 by SBFI-26, however, did not induce dependence, cognitive impairments, or peripheral side effects (Thanos et al. 2016). Our results add further evidence on safety and tolerability of FABP-5 inhibition, suggesting that local inhibition of FABP-5 in the brain does not impair locomotion, memory, or sensorimotor gating. Additionally, our finding that acute FABP-5 inhibition had no impact on baseline dopamine system activity states further suggests that this novel mechanism can produce effective anxiolytic effects whilst bypassing the mesolimbic dopamine system, posing less risk for activation of addiction-related brain pathways. Despite its promising therapeutic activity and safety profile, we should note that SBFI-103 remains to be validated for its translatability to humans as well as testing in other preclinical animal models. In addition, the present studies focused on intracranial infusions and future studies are required using systemic administration in order to confirm its safety and tolerability in human patients. Furthermore, future studies are required to address potential off-target side effects of SBFI-103, especially on dependence, withdrawal and various aspects of cognition and memory.

Anxiety and fear are both adaptive responses to evade threats, and although their neural circuitries overlap regarding neuroanatomy and neurotransmitters/neuromodulators, there are clear distinctions between fear and anxiety in terms of cause and effect as well as their underlying neurobiological mechanism (Wang et al. 2011; Perusini and Fanselow 2015). Preclinical findings have demonstrated a significant role of eCBs and CB1R in the behavioral adaptation of fear responses (Laviolette and Grace 2006). Systemic administration of agents that elevate eCB neurotransmission has been shown to suppress fear expression and facilitate fear extinction in rodents (Marsicano et al. 2002; Chhatwal et al. 2005; Gunduz-Cinar, MacPherson, et al. 2013a) and humans (Mayo et al. 2020). Furthermore, intracerebroventricular infusion of agents that elevate eCB neurotransmission, or their local infusion into the mPFC or BLA prior to memory retention tests, promotes extinction of cued and contextual fear, which was dependent on CB1R (Bitencourt et al. 2008; Lin et al. 2009; Gunduz-Cinar, MacPherson, et al. 2013a). Systemic antagonism of CB1R, also, has been shown to impact contextual fear expression (Suzuki et al. 2004) as well as fear

generalization (Reich et al. 2008). Although we did not directly investigate CB1R antagonism in the absence of SBFI-103, our results are in line with these findings and may indicate the involvement of CB1R transmission in both contextual fear expression and fear-memory generalization behaviors. CB1R-mediated effects on cortical neurons seem to exert control on behaviors only when environmental aversiveness exceeds an arbitrary threshold (Haller et al. 2004; Hölter et al. 2005; Carnevali et al. 2017). As our fear conditioning paradigm used a suprathreshold aversion stimulus, it possibly rendered the neutral, novel environment aversive, causing a CB1R-dependent generalized fear response. CB2R, despite not having been as thoroughly investigated, has also been shown to be involved in the modulation of fear responses (Ten-Blanco et al. 2022). For example, genetic ablation of CB2R impaired contextual fear memories in mice (Li and Kim 2016). Importantly, exposing rats to trimethylthiazoline, a molecular component of a predator odor, increased the transcription of *Cnr2* gene (which encodes for CB2R in rodents) in rat PFC (Ivy et al. 2020), which possibly enhances stress-coping behaviors. Finally, a functional polymorphism on the *Cnr2* gene, which impairs CB2R activity, has been associated with the pathogenesis of post-traumatic stress disorder (Lazary et al. 2019), again indicating the involvement of CB2R in adaptive fear expression.

Although the involvement of CB1R-mediated eCB neurotransmission in the expression of fear is well-established in the literature (Lin et al. 2009), there are conflicting reports about its involvement in anxiety-like behaviors (Lutz et al. 2015). For example, some findings suggest that while CB1R antagonism or its genetic ablation could modulate emotional behavior, these effects may only be limited to conditions of high environmental stress (Haller et al. 2004; Hölter et al. 2005; Carnevali et al. 2017). Such stressful environments, leading to the formation of behavioral coping strategies, could be more reliably examined with behavioral measures of fear rather than anxiety, because behavioral tests measuring fear in rodents are unavoidably stressful and aversive, whereas during the behavioral tests measuring anxiety, animals can simply evade the aversive and stressful environment. Furthermore, both glutamatergic and GABAergic presynaptic neurons express CB1R (Kano et al. 2009). Therefore, the emergence of anxiolytic or anxiogenic responses can depend on whether eCB-activated CB1Rs are expressed on glutamatergic or GABAergic neurons. Our findings are in line with reports associating CB1R-mediated FABP-5 signaling pathway with the expression of fear, but not with anxiety-like behavior, which instead depended on CB2R-mediated FABP-5 signaling pathway. This suggests a novel CB2-dependent anxiety processing mechanism directly in the PLC.

Although earlier studies suggested a lack of functional CB2R expression in healthy brain (Munro et al. 1993; Griffin et al. 1999; Benito et al. 2003), recent imaging

studies reported brain-wide neuronal and glial CB2R expression, including the mPFC (Onaivi et al. 2012; Jordan and Xi 2019). Disrupted CB2R activity was linked with the pathophysiology of schizophrenia, depression, and anxiety disorders (Onaivi et al. 2008; Ishiguro et al. 2010; Ortega-Alvaro et al. 2011; Li and Kim 2017), while CB2R overexpression with a depression-resistant phenotype (García-Gutiérrez et al. 2010) and decreased vulnerability to anxiety in mice (García-Gutiérrez and Manzanares 2011). Importantly, unlike CB1R, CB2R activation opens postsynaptic calcium-activated chloride channels in rodent mPFC, leading to reduced neuronal excitability and reduced firing frequency in layer II/III pyramidal cells (Den Boon et al. 2012). FABP-5 inhibition-induced CB2R activation, employing this mechanism, might underlie the behavioral and physiological action of SBFI-103, and explain why the anxiolytic-like effects of SBFI-103 are reversed by CB2R, but not CB1R, antagonism. We also demonstrate that GPR55-mediated neurotransmission is involved in the expression of anxiety. In HEK293 cells, CB2R and GPR55 have been shown to interact and form functional heteromers, which modulate activation of various transcription factors and signaling pathways, most notably the extracellular signal-regulated kinase (Erk) 1/2 (Balenga et al. 2014). Furthermore, the expression of CB2R-GPR55 heteromers is elevated in the dorsolateral PFC of suicide victims (García-Gutiérrez et al. 2018), possibly as a compensatory alteration. Thus, a CB2R-GPR55 heteromer-mediated mechanism might underlie the anxiolytic effects of FABP-5 inhibition.

The mPFC, BLA, and VHipp form a tripartite circuit regulating fear and anxiety-related behaviors. The mPFC exerts top-down control and drives BLA neurons that preferentially project to mPFC and VHipp to form a connected circuitry, which selects appropriate behavioral adaptation and coping strategies to fearful and/or potentially dangerous environmental stimuli (Sotres-Bayon et al. 2012; Felix-Ortiz et al. 2013; McGarry and Carter 2017). Furthermore, monosynaptic inputs from VHipp to mPFC are believed to be a key component of this circuitry, conveying contextual information for context-unconditioned stimulus associations and modulating anxiety-related behavior by representing aversive information (Adhikari et al. 2010; Kim and Cho 2017). The anxiolytic and fear-inhibiting actions of FABP-5 inhibition could act on this circuitry to exert its behavioral effects. Using electrophysiological recordings, we demonstrated attenuated firing activity of BLA putative principal neurons and elevated firing of VHipp putative pyramidal neurons after intra-PLC FABP-5 inhibition. Intra-PLC FABP-5 inhibition may therefore activate CB2Rs in the mPFC to reduce excitability of glutamatergic neurons projecting to BLA, dampening its activity. Nonspecific activation of projection neurons in the BLA was shown to induce anxiety-like behavior, whereas their inactivation was anxiolytic (Janak and Tye 2015), similar to specific activation/inactivation of BLA efferents in VHipp

(Janak and Tye 2015), and supporting our findings. Furthermore, humans with high trait-anxiety and post-traumatic stress disorder (PTSD) show elevated BLA activation to fear cues (Shin et al. 2005; Indovina et al. 2011). As the firing of BLA projection neurons is reduced by intra-PLC FABP-5 inhibition, excitatory monosynaptic BLA → VHipp projections should also be reduced, yet we detected elevated firing of VHipp principal neurons. As the majority of BLA projection neurons are excitatory, a disinhibitory effect of GABAergic interneurons in the VHipp could explain this inconsistency. Interestingly, VHipp efferents in the BLA preferentially activate GABAergic interneurons resulting in dampened activity of principal BLA neurons (Janak and Tye 2015), corroborating our results correlating increased VHipp activity with decreased BLA firing.

Synchronized oscillatory activity between VHipp-mPFC and VHipp-BLA is elevated during the expression of fear and anxiety (Çalışkan and Stork 2018). In the VHipp, exposure to anxiogenic environments increases theta and gamma power (Adhikari et al. 2010; Çalışkan and Stork 2018). However, in these studies, definition of theta oscillations was 4–12 Hz, which corresponds to our theta (4–7 Hz) and most of the alpha (7–14 Hz) band. With this difference in mind, FABP-5 inhibition decreased the power of alpha, and low gamma oscillations in the VHipp, which might help overcome the anxiety-inducing aversiveness of conditioned fear environments. In the BLA, mPFC theta activity drives gamma oscillations in the BLA during fear processing (Stujenske et al. 2014). Furthermore, in the BLA, safety signals have been shown to increase gamma power, whereas fear signals attenuate it (Stujenske et al. 2014). These reports, together with our findings indicate that elevated BLA gamma oscillations may be involved in the suppression of fear and anxiety-related behaviors.

While the present study focused on the behavioral and electrophysiological effects as well as the safety of intra-PLC inhibition of FABP-5, it is important to note that the therapeutic efficacy and tolerability of systemic FABP-5 inhibition remains unknown, which limits its translational potential. Furthermore, although we believe that FABP-5 inhibition-induced behavioral and neurophysiological effects are mediated by elevated AEA-mediated neurotransmission, AEA quantification has not been performed in the PLC, which is a major limitation in this study. Finally, only male animals have been used in this study, thus, the therapeutic effects and tolerability of FABP-5 inhibition should also be tested in female animals. Future studies are required to address these limitations.

In summary, our findings identify a novel CB2R-dependent FABP-5 signaling pathway in the mPFC, which modulates anxiety, fear expression, and neuronal transmission patterns. This data suggests that the prefrontal cortical FABP-5 system may serve as a promising target for the development of novel anxiolytic interventions. Additionally, our findings that

intra-mPFC inhibition of FABP-5 can reduce anxiety-related behaviors in the absence of cognitive side-effects or modulation of dopaminergic signaling pathways, further identify this FABP-5-CB2R dependent mechanism as a promising alternative to traditional anxiolytic compounds.

Supplementary material

Supplementary material is available at *Cerebral Cortex* online.

Authors' contributions

TCU, SRL designed the research study. TCU performed the surgeries and behavioral experiments with the assistance of HJS and MJJ. TCU performed the electrophysiological experiments with the assistance of HJS and MGN. TCU analyzed the data. MJJ performed histology. TC and IO synthesized and provided SBFI-103. WJR and SRL contributed essential reagents and equipment. TCU and SRL wrote the manuscript. All authors revised the manuscript.

Funding

This work was supported by Artelo Biosciences and MITACs CANADA, and by a grant (DA035923 (to IO) from the National Institutes of Health, USA.

Conflict of interest statement: The authors declare that they have no competing financial interests.

References

- Adhikari A, Topiwala MA, Gordon JA. Synchronized activity between the ventral hippocampus and the medial prefrontal cortex during anxiety. *Neuron*. 2010;65:257–269.
- Alger BE, Kim J. Supply and demand for endocannabinoids. *Trends Neurosci*. 2011;34:304.
- Balenga NA, Martínez-Pinilla E, Kargl J, Schröder R, Peinhaupt M, Platzer W, Bálint Z, Zamarbidé M, Dopeso-Reyes IG, Ricobaraza A, et al. Heteromerization of GPR55 and cannabinoid CB2 receptors modulates signalling. *Br J Pharmacol*. 2014;171:5387–5406.
- Benito C, Núñez E, Tolón RM, Carrier EJ, Rábano A, Hillard CJ, Romero J. Cannabinoid CB2 receptors and fatty acid amide hydrolase are selectively overexpressed in neuritic plaque-associated glia in Alzheimer's disease brains. *J Neurosci*. 2003;23:11136–11141.
- Bitencourt RM, Pamplona FA, Takahashi RN. Facilitation of contextual fear memory extinction and anti-anxiogenic effects of AM404 and cannabidiol in conditioned rats. *Eur Neuropsychopharmacol*. 2008;18:849–859.
- Blankman JL, Cravatt BF. Chemical probes of endocannabinoid metabolism. *Pharmacol Rev*. 2013;65:849–871.
- Çalışkan G, Stork O. Hippocampal network oscillations at the interplay between innate anxiety and learned fear. *Psychopharmacol*. 2018;236:321–338.
- Carnevali L, Rivara S, Nalivaiko E, Thayer JF, Vacondio F, Mor M, Sgoifo A. Pharmacological inhibition of FAAH activity in rodents:

- A promising pharmacological approach for psychological-cardiac comorbidity? *Neurosci Biobehav Rev.* 2017;74:444–452.
- Chhatwal JP, Davis M, Maguschak KA, Ressler KJ. Enhancing cannabinoid neurotransmission augments the extinction of conditioned fear. *Neuropsychopharmacology.* 2005;30:516–524.
- Cravatt BF, Demarest K, Patricelli MP, Bracey MH, Giang DK, Martin BR, Lichtman AH. Supersensitivity to anandamide and enhanced endogenous cannabinoid signaling in mice lacking fatty acid amide hydrolase. *Proc Natl Acad Sci U S A.* 2001;98:9371–9376.
- De Felice M, Renard J, Hudson R, Szkudlarek HJ, Pereira BJ, Schmid S, Rushlow WJ, Laviolette SR. L-theanine prevents long-term affective and cognitive side effects of adolescent Δ -9-tetrahydrocannabinol exposure and blocks associated molecular and neuronal abnormalities in the mesocorticolimbic circuitry. *J Neurosci.* 2021;41:739–750.
- Den Boon FS, Chameau P, Schaafsma-Zhao Q, Van Aken W, Bari M, Oddi S, Kruse CG, Maccarrone M, Wadman WJ, Werkmana TR. Excitability of prefrontal cortical pyramidal neurons is modulated by activation of intracellular type-2 cannabinoid receptors. *Proc Natl Acad Sci U S A.* 2012;109:3534–3539.
- Dincheva I, Drysdale AT, Hartley CA, Johnson DC, Jing D, King EC, Ra S, Gray JM, Yang R, DeGruccio AM, et al. FAAH genetic variation enhances fronto-amygdala function in mouse and human. *Nat Commun.* 2015;6:1–9.
- Felix-Ortiz AC, Beyeler A, Seo C, Leppla CA, Wildes CP, Tye KM. BLA to vHPC inputs modulate anxiety-related behaviors. *Neuron.* 2013;79:658–664.
- Figueiredo A, Hamilton J, Marion M, Blum K, Kaczocha M, Haj-Dahmane S, Deutsch D, Thanos PK. Pharmacological inhibition of brain fatty acid binding protein reduces ethanol consumption in mice. *J Reward Defic Syndr Addict Sci.* 2017;3:21–27.
- Fowler CJ. Transport of endocannabinoids across the plasma membrane and within the cell. *FEBS J.* 2013;280:1895–1904.
- Garani R, Watts JJ, Mizrahi R. Endocannabinoid system in psychotic and mood disorders, a review of human studies. *Prog Neuro-Psychopharmacol Biol Psychiatry.* 2021;106:110096.
- García-Gutiérrez MS, Manzanares J. Overexpression of CB2 cannabinoid receptors decreased vulnerability to anxiety and impaired anxiolytic action of alprazolam in mice. *J Psychopharmacol.* 2011;25:111–120.
- García-Gutiérrez MS, Pérez-Ortiz JM, Gutiérrez-Adán A, Manzanares J. Depression-resistant endophenotype in mice overexpressing cannabinoid CB2 receptors. *Br J Pharmacol.* 2010;160:1773–1784.
- García-Gutiérrez MS, Navarrete F, Navarro G, Reyes-Resina I, Franco R, Lanciego JL, Giner S, Manzanares J. Alterations in gene and protein expression of cannabinoid CB2 and GPR55 receptors in the dorsolateral prefrontal cortex of suicide victims. *Neurotherapeutics.* 2018;15:796–806.
- Griebel G, Holmes A. 50 years of hurdles and hope in anxiolytic drug discovery. *Nat Rev Drug Discov.* 2013;12:667–687.
- Griffin G, Wray EJ, Tao Q, McAllister SD, Rorrer WK, Aung M, Martin BR, Abood ME. Evaluation of the cannabinoid CB2 receptor-selective antagonist, SR144528: further evidence for cannabinoid CB2 receptor absence in the rat central nervous system. *Eur J Pharmacol.* 1999;377:117–125.
- Gunduz-Cinar O, MacPherson KP, Cinar R, Gamble-George J, Sugden K, Williams B, Godlewski G, Ramikie TS, Gorka AX, Alapafuja SO, et al. Convergent translational evidence of a role for anandamide in amygdala-mediated fear extinction, threat processing and stress-reactivity. *Mol Psychiatry.* 2013a;18:813–823.
- Gunduz-Cinar O, Hill MN, McEwen BS, Holmes A. Amygdala FAAH and anandamide: mediating protection and recovery from stress. *Trends Pharmacol Sci.* 2013b;34:637–644.
- Haller J, Varga B, Ledent C, Barna I, Freund TF. Context-dependent effects of CB1 cannabinoid gene disruption on anxiety-like and social behaviour in mice. *Eur J Neurosci.* 2004;19:1906–1912.
- Hamilton J, Koumas C, Clavin BH, Marion M, Figueiredo A, Gonzalez S, O'Rourke JR, Deutsch D, Kaczocha M, Haj-Dahmane S, et al. Fatty acid-binding proteins 5 and 7 gene deletion increases sucrose consumption and diminishes forced swim immobility time. *Behav Pharmacol.* 2018;29:503–508.
- Hariri AR, Gorka A, Hyde LW, Kimak M, Halder I, Ducci F, Ferrell RE, Goldman D, Manuck SB. Divergent effects of genetic variation in endocannabinoid signaling on human threat- and reward-related brain function. *Biol Psychiatry.* 2009;66:9–16.
- Hill MN, Kumar SA, Filipinski SB, Iverson M, Stuhr KL, Keith JM, Cravatt BF, Hillard CJ, Chattarji S, McEwen BS. Disruption of fatty acid amide hydrolase activity prevents the effects of chronic stress on anxiety and amygdalar microstructure. *Mol Psychiatry.* 2013;18:1125–1135.
- Hölter SM, Kallnik M, Wurst W, Marsicano G, Lutz B, Wotjak CT. Cannabinoid CB1 receptor is dispensable for memory extinction in an appetitively-motivated learning task. *Eur J Pharmacol.* 2005;510:69–74.
- Indovina I, Robbins TW, Núñez-Elizalde AO, Dunn BD, Bishop SJ. Fear-conditioning mechanisms associated with trait vulnerability to anxiety in humans. *Neuron.* 2011;69:563–571.
- Ishiguro H, Horiuchi Y, Ishikawa M, Koga M, Imai K, Suzuki Y, Morikawa M, Inada T, Watanabe Y, Takahashi M, et al. Brain cannabinoid CB2 receptor in schizophrenia. *Biol Psychiatry.* 2010;67:974–982.
- Ivy D, Palese F, Vozella V, Fotio Y, Yalcin A, Ramirez G, Mears D, Wynn G, Piomelli D. Cannabinoid CB2 receptors mediate the anxiolytic-like effects of monoacylglycerol lipase inhibition in a rat model of predator-induced fear. *Neuropsychopharmacology.* 2020;45:1330–1338.
- Janak PH, Tye KM. From circuits to behaviour in the amygdala. *Nature.* 2015;517:284–292.
- Jordan CJ, Xi ZX. Progress in brain cannabinoid CB2 receptor research: from genes to behavior. *Neurosci Biobehav Rev.* 2019;98:208–220.
- Kaczocha M, Glaser ST, Deutsch DG. Identification of intracellular carriers for the endocannabinoid anandamide. *Proc Natl Acad Sci U S A.* 2009;106:6375–6380.
- Kaczocha M, Rebecchi MJ, Ralph BP, Teng YHG, Berger WT, Galbavy W, Elmes MW, Glaser ST, Wang L, Rizzo RC, et al. Inhibition of fatty acid binding proteins elevates brain anandamide levels and produces analgesia. *PLoS One.* 2014;9:1–10.
- Kaczocha M, Glaser ST, Maher T, Clavin B, Hamilton J, O'Rourke J, Rebecchi M, Puopolo M, Owada Y, Thanos PK. Fatty acid binding protein deletion suppresses inflammatory pain through endocannabinoid/N-acylethanolamine-dependent mechanisms. *Mol Pain.* 2015;11:52.
- Kano M, Ohno-Shosaku T, Hashimoto-dani Y, Uchigashima M, Watanabe M. Endocannabinoid-mediated control of synaptic transmission. *Physiol Rev.* 2009;89:309–380.
- Kathuria S, Gaetani S, Fegley D, Valiño F, Duranti A, Tontini A, Mor M, Tarzia G, La Rana G, Calignano A, et al. Modulation of anxiety through blockade of anandamide hydrolysis. *Nat Med.* 2003;9:76–81.
- Kim WB, Cho JH. Synaptic targeting of double-projecting ventral CA1 hippocampal neurons to the medial prefrontal cortex and basal amygdala. *J Neurosci.* 2017;37:4868–4882.

- Kim EJ, Kim N, Kim HT, Choi JS. The prefrontal cortex is critical for context-dependent fear expression. *Front Behav Neurosci*. 2013;7:1–15.
- Kramar C, Loureiro M, Renard J, Laviolette SR. Palmitoylethanolamide modulates GPR55 receptor signaling in the ventral hippocampus to regulate mesolimbic dopamine activity, social interaction, and memory processing. *Cannabis Cannabinoid Res*. 2017;2:8–20.
- Laviolette SR. Exploring the impact of adolescent exposure to cannabinoids and nicotine on psychiatric risk: insights from translational animal models. *Psychol Med*. 2021;51:940–947.
- Laviolette SR, Grace AA. The roles of cannabinoid and dopamine receptor systems in neural emotional learning circuits: implications for schizophrenia and addiction. *Cell Mol Life Sci*. 2006;63:1597–1613.
- Lazary J, Eszlari N, Juhasz G, Bagdy G. A functional variant of CB2 receptor gene interacts with childhood trauma and FAAH gene on anxious and depressive phenotypes. *J Affect Disord*. 2019;257:716–722.
- Li Y, Kim J. CB2 cannabinoid receptor knockout in mice impairs contextual long-term memory and enhances spatial working memory. *Neural Plast*. 2016;2016:9817089.
- Li Y, Kim J. Distinct roles of neuronal and microglial CB2 cannabinoid receptors in the mouse hippocampus. *Neuroscience*. 2017;363:11–25.
- Li GL, Winter H, Arends R, Jay GW, Le V, Young T, Huggins JP. Assessment of the pharmacology and tolerability of PF-04457845, an irreversible inhibitor of fatty acid amide hydrolase-1, in healthy subjects. *Br J Clin Pharmacol*. 2012;73:706–716.
- Lin HC, Mao SC, Su CL, Gean PW. The role of prefrontal cortex CB1 receptors in the modulation of fear memory. *Cereb Cortex*. 2009;19:165–175.
- Lisboa SF, Borges AA, Nejo P, Fassini A, Guimarães FS, Resstel LB. Cannabinoid CB1 receptors in the dorsal hippocampus and prefrontal medial prefrontal cortex modulate anxiety-like behavior in rats: additional evidence. *Prog Neuro-Psychopharmacol Biol Psychiatry*. 2015;59:76–83.
- Locci A, Pinna G. Stimulation of peroxisome proliferator-activated receptor- α by N-palmitoylethanolamine engages allopregnanolone biosynthesis to modulate emotional behavior. *Biol Psychiatry*. 2019;85(12):1036–1045.
- Loureiro M, Kramar C, Renard J, Rosen LG, Laviolette SR. Cannabinoid transmission in the hippocampus activates nucleus accumbens neurons and modulates reward and aversion-related emotional salience. *Biol Psychiatry*. 2016;80:216–225.
- Lutz B, Marsicano G, Maldonado R, Hillard CJ. The endocannabinoid system in guarding against fear, anxiety and stress. *Nat Rev Neurosci*. 2015;16:705–718.
- Marsicano G, Wotjak CT, Azad SC, Bisogno T, Rammes G, Cascioli MG, Hermann H, Tang J, Hofmann C, Zieglgänsberger W, et al. The endogenous cannabinoid system controls extinction of aversive memories. *Nature*. 2002;418:530–534.
- Marsicano G, Goodenough S, Monory K, Hermann H, Eder M, Cannich A, Azad SC, Cascio MG, Ortega-Gutiérrez S, Van der Stelt M, et al. CB1 cannabinoid receptors and on-demand defense against excitotoxicity. *Science*. 2003;302:84–88.
- Mayo LM, Asratian A, Lindé J, Morena M, Haataja R, Hammar V, Augier G, Hill MN, Heilig M. Elevated anandamide, enhanced recall of fear extinction, and attenuated stress responses following inhibition of fatty acid amide hydrolase: a randomized, controlled experimental medicine trial. *Biol Psychiatry*. 2020;87:538–547.
- McGarry LM, Carter AG. Prefrontal cortex drives distinct projection neurons in the basolateral amygdala. *Cell Rep*. 2017;21:1426–1433.
- Munro S, Thomas KL, Abu-Shaar M. Molecular characterization of a peripheral receptor for cannabinoids. *Nature*. 1993;365:61–65.
- Norris C, Szkudlarek HJ, Pereira B, Rushlow W, Laviolette SR. The bivalent rewarding and aversive properties of Δ^9 -tetrahydrocannabinol are mediated through dissociable opioid receptor substrates and neuronal modulation mechanisms in distinct striatal sub-regions. *Sci Rep*. 2019;9:1–14.
- Onaivi ES, Ishiguro H, Gong J-P, Patel S, Meozzi PA, Myers L, Perchuk A, Mora Z, Tagliaferro PA, Gardner E, et al. Brain neuronal CB2 cannabinoid receptors in drug abuse and depression: from mice to human subjects. *PLoS One*. 2008;3:e1640.
- Onaivi ES, Ishiguro H, Gu S, Liu Q-R. CNS effects of CB2 cannabinoid receptors: beyond neuro-immuno-cannabinoid activity. *J Psychopharmacol*. 2012;26:92–103.
- Ortega-Alvaro A, Aracil-Fernández A, García-Gutiérrez MS, Navarrete F, Manzanares J. Deletion of CB2 cannabinoid receptor induces schizophrenia-related behaviors in mice. *Neuropsychopharmacology*. 2011;36:1489–1504.
- Owada Y, Yoshimoto T, Kondo H. Spatio-temporally differential expression of genes for three members of fatty acid binding proteins in developing and mature rat brains. *J Chem Neuroanat*. 1996;12:113–122.
- Paxinos G, Watson C. *The rat brain in stereotaxic coordinates*. Hard Cover Edition. Academic Press, San Diego; 2013.
- Peng X, Studholme K, Kanjiya MP, Luk J, Bogdan D, Elmes MW, Carbonetti G, Tong S, Teng GYH, Rizzo RC, et al. Fatty-acid-binding protein inhibition produces analgesic effects through peripheral and central mechanisms. *Mol Pain*. 2017;13:1744806917697007.
- Perusini JN, Fanselow MS. Neurobehavioral perspectives on the distinction between fear and anxiety. *Learn Mem*. 2015;22:417–425.
- Poulos AM, Mehta N, Lu B, Amir D, Livingston B, Santarelli A, Zhuravka I, Fanselow MS. Conditioning- and time-dependent increases in context fear and generalization. *Learn Mem*. 2016;23:379–385.
- Reich CG, Mohammadi MH, Alger BE. Endocannabinoid modulation of fear responses: learning and state-dependent performance effects. *J Psychopharmacol*. 2008;22:769–777.
- Renard J, Szkudlarek HJ, Kramar CP, Jobson CEL, Moura K, Rushlow WJ, Laviolette SR. Adolescent THC exposure causes enduring prefrontal cortical disruption of GABAergic inhibition and dysregulation of sub-cortical dopamine function. *Sci Rep*. 2017;7:1–14.
- Shimamoto C, Ohnishi T, Maekawa M, Watanabe A, Ohba H, Arai R, Iwayama Y, Hisano Y, Toyota T, Toyoshima M, et al. Functional characterization of FABP3, 5 and 7 gene variants identified in schizophrenia and autism spectrum disorder and mouse behavioral studies. *Hum Mol Genet*. 2014;23:6495–6511.
- Shin LM, Wright CI, Cannistraro PA, Wedig MM, McMullin K, Martis B, Macklin ML, Lasko NB, Cavanagh SR, Krangel TS, et al. A functional magnetic resonance imaging study of amygdala and medial prefrontal cortex responses to overtly presented fearful faces in posttraumatic stress disorder. *Arch Gen Psychiatry*. 2005;62:273–281.
- Smathers RL, Petersen DR. The human fatty acid-binding protein family: evolutionary divergences and functions. *Hum Genomics*. 2011;5:1–22.
- Sotres-Bayon F, Sierra-Mercado D, Pardilla-Delgado E, Quirk GJ. Gating of fear in prefrontal cortex by hippocampal and amygdala inputs. *Neuron*. 2012;76:804–812.
- Stujenske JM, Likhtik E, Topiwala M, Gordon JA. Fear and safety engage competing patterns of theta-gamma coupling in the basolateral amygdala. *Neuron*. 2014;83:919–933.

- Suzuki A, Josselyn SA, Frankland PW, Masushige S, Silva AJ, Kida S. Memory reconsolidation and extinction have distinct temporal and biochemical signatures. *J Neurosci*. 2004;24:4787–4795.
- Szkudlarek HJ, Desai SJ, Renard J, Pereira B, Norris C, Jobson CEL, Rajakumar N, Allman BL, Laviolette SR. Δ -9-tetrahydrocannabinol and cannabidiol produce dissociable effects on prefrontal cortical executive function and regulation of affective behaviors. *Neuropsychopharmacology*. 2019;44:817–825.
- Tan H, Lauzon NM, Bishop SF, Chi N, Bechard M, Laviolette SR. Cannabinoid transmission in the basolateral amygdala modulates fear memory formation via functional inputs to the prelimbic cortex. *J Neurosci*. 2011;31:5300–5312.
- Ten-Blanco M, Flores A, Pereda-Perez I, Piscitelli F, Izquierdo-Luengo C, Cristino L, Romero J, Hillard CJ, Maldonado R, Di Marzo V, et al. Amygdalar CB2 cannabinoid receptor mediates fear extinction deficits promoted by orexin-A/hypocretin-1. *Biomed Pharmacother*. 2022;149:112925.
- Thanos PK, Clavin BH, Hamilton J, O'Rourke JR, Maher T, Koumas C, Miao E, Lankop J, Elhage A, Haj-Dahmane S, et al. Examination of the addictive and behavioral properties of fatty acid-binding protein inhibitor SBFI26. *Front Psychiatry*. 2016;7:4–10.
- Tourão C, Oveisi F, Lockney J, Piomelli D, Maldonado R. FAAH deficiency promotes energy storage and enhances the motivation for food. *Int J Obes*. 2010;34:557–568.
- Wang DV, Wang F, Liu J, Zhang L, Wang Z, Lin L. Neurons in the amygdala with response-selectivity for anxiety in two ethologically based tests. *PLoS One*. 2011;6:e18739.
- Yan S, Elmes MW, Tong S, Hu K, Awwa M, Teng GYH, Jing Y, Freitag M, Gan Q, Clement T, et al. SAR studies on truxillic acid mono esters as a new class of antinociceptive agents targeting fatty acid binding proteins. *Eur J Med Chem*. 2018;154:233–252.
- Yu S, Levi L, Casadesus G, Kunos G, Noy N. Fatty acid-binding protein 5 (FABP5) regulates cognitive function both by decreasing anandamide levels and by activating the nuclear receptor peroxisome proliferator-activated receptor α/β (PPAR α/β) in the brain. *J Biol Chem*. 2014;289:12748–12758.
- Zaitone SA, El-Wakeil AF, Abou-El-Ela SH. Inhibition of fatty acid amide hydrolase by URB597 attenuates the anxiolytic-like effect of acetaminophen in the mouse elevated plus-maze test. *Behav Pharmacol*. 2012;23:417–425.
- Zhang HY, Gao M, Liu QR, Bi GH, Li X, Yang HJ, Gardner EL, Wu J, Xi ZX. Cannabinoid CB2 receptors modulate midbrain dopamine neuronal activity and dopamine-related behavior in mice. *Proc Natl Acad Sci U S A*. 2014;111:E5007–E5015.
- Zhang LY, Zhou YQ, Yu ZP, Zhang XQ, Shi J, Shen HW. Restoring glutamate homeostasis in the nucleus accumbens via endocannabinoid-mimetic drug prevents relapse to cocaine seeking behavior in rats. *Neuropsychopharmacology*. 2021;46:970–981.